$$F_2 = \begin{bmatrix} \dfrac{1}{3} & -\dfrac{1}{3\sqrt{6}} & \dfrac{1}{3\sqrt{3}} \\ 0 & 0 & 0 \\ \dfrac{1}{\sqrt{3}} & -\dfrac{1}{3\sqrt{2}} & \dfrac{1}{3} \end{bmatrix} \qquad [31]$$

In evaluating the final deformation gradient matrix $e^{\alpha F_1}$ (Eq. [21]) by the use of Eqs. [22] to [24], the procedure is straightforward and can be found in standard texts. The elements of the diagonal matrix Λ (Eq. [22]) are found to be $\lambda_1 = -2/\sqrt{6}$, $\lambda_2 = 0$, $\lambda_3 = 2/\sqrt{6}$, and suitable matrices for the similarity transformation of Eqs. [22] and [23] are

$$S = \begin{bmatrix} 1 & 0 & 0 \\ 0 & 1 & 0 \\ 0 & -\dfrac{1}{\sqrt{2}} & 1 \end{bmatrix}, \quad S^{-1} = \begin{bmatrix} 1 & 0 & 0 \\ 0 & 1 & 0 \\ 0 & \dfrac{1}{\sqrt{2}} & 1 \end{bmatrix} \quad [32]$$

The application of Eqs. [23] and [24] then leads to the desired deformation gradient matrix

$$F = e^{\alpha F_1} = S^{-1} \begin{bmatrix} e^{-\varphi} & 0 & 0 \\ 0 & 1 & 0 \\ 0 & -\dfrac{1}{\sqrt{2}} e^{\varphi} & e^{\varphi} \end{bmatrix}$$

$$= \begin{bmatrix} e^{-\varphi} & 0 & 0 \\ 0 & 1 & 0 \\ 0 & \dfrac{1}{\sqrt{2}}(1 - e^{\varphi}) & e^{\varphi} \end{bmatrix} \qquad [33]$$

where we have substituted $\varphi \equiv 2\alpha/\sqrt{6}$ merely as an abbreviation.

To obtain the formulas relating the changes in specimen dimensions and angles of lines, it may be shown that application of Eqs. [5] to [7] and [33] leads to values of

$$\frac{h_1}{h_0} = e^{-\varphi}$$

$$\frac{w_1}{w_0} = 1$$

$$\frac{l_1}{l_0} = e^{\varphi} \qquad\qquad [34]$$

$$\tan \theta_{32} = \frac{1}{\sqrt{2}}(1 - e^{\varphi})$$

where h_1, w_1, l_1 and h_0, w_0, l_0 refer to specimen height, width, and length after and before the deformation, respectively, and θ_{32} is the angle by which a line originally parallel to the $[\bar{1}1\bar{1}]$ direction has shifted in the $[\bar{1}12]$ direction.

By contrast, it can be shown that the use of infinitesimal strain equations [3] leads to the following expressions:

$$\frac{h_1}{h_0} = 1 - \varphi$$

$$\frac{w_1}{w_0} = 1$$

$$\frac{l_1}{l_0} = 1 + \varphi$$

$$\tan \theta_{32} = -\frac{\sqrt{2}}{2}\varphi \qquad [35]$$

which may also be deduced from Eq. [34] for *small* values of φ. Clearly for large values of φ, Eq. [35] can be quite erroneous.

Experiment. A single crystal of Permalloy (4 pct Mo-17 pct Fe-79 pct Ni) was compressed on the (110) plane with the elongation confined to the $[\bar{1}12]$ direction. A special compression die was constructed to restrict lateral spreading of the specimen. As illustrated in Fig. 3, the die consists of a slot formed by three steel blocks bolted together to facilitate specimen removal. After the sample is placed in the slot a plunger is fitted on top and the ensemble placed in a Baldwin hydraulic machine for compression testing. Good lubrication was achieved with 5-mil-thick Teflon strips. Periodically the sample was removed for dimensional measurement as well as for renewal of the Teflon. A more detailed description of the experiment is given in Ref. 7.

The specimen shape after a 50.5 pct reduction in height is shown in Fig. 4. Metallographic observations of the slip-line tracings indicate that slip had occurred primarily on the two expected systems (111)[10$\bar{1}$] and (11$\bar{1}$)[011], Fig. 5. From Eq. [34] one obtains

$$\tan \theta_{32} = \frac{1}{\sqrt{2}}\left(1 - \frac{h_0}{h_1}\right) \qquad [36]$$
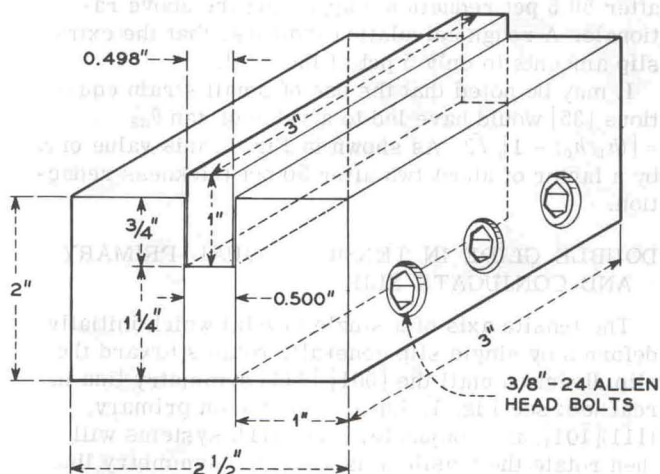

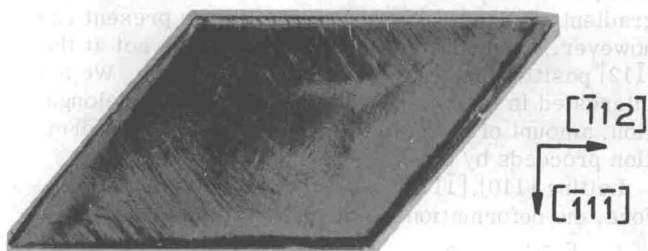Fig. 3—Compression device for approximating constrained deformation.

Fig. 4—Top view of Permalloy single crystal compressed on (110) plane and elongated in $[\bar{1}12]$ direction. Thickness reduction 50.5 pct. Initial rectangular shape has changed to a parallelogram. Directions noted in margins. X2.70. Reduced approximately 1 pct for reproduction.
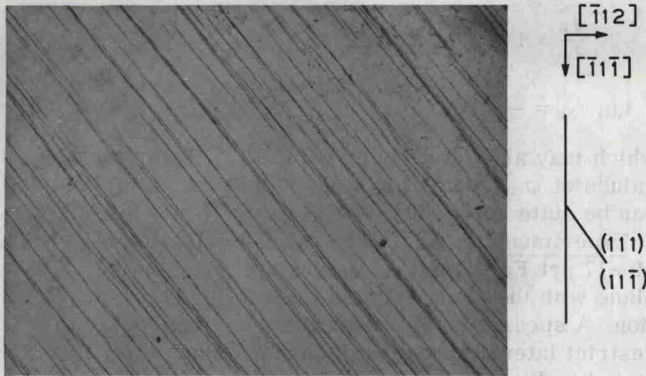
(111)
(11$\bar{1}$)

Fig. 5—Slip traces on top surface of (110)[$\bar{1}12$] Permalloy crystal. Compressed 50.5 pct, electropolished, and then lightly compressed. Traces correspond to both (111) and (11$\bar{1}$) slip planes. X140. Reduced approximately 34 pct for reproduction.

and hence a plot of $\tan \theta_{32}$ vs $(1 - h_0/h_1)$ should yield a straight line with a slope of 0.707. This is shown in Fig. 6, together with the experimentally determined points. Agreement is considered very good. The slight positive deviation from the expected line can be explained on the basis of a small activity on the systems (111)[$01\bar{1}$] and (11$\bar{1}$)[101]; see Fig. 2. If lateral constraint had been absent, all four slip systems would have been equally favored. It can be shown that slip on (111)[$01\bar{1}$] and (11$\bar{1}$)[101] systems will cause lateral spreading as well as contributing to a larger value of θ_{32}. The measured width of the sample was found to increase from 0.498 to 0.509 in. after 50.5 pct reduction, supporting the above rationale. A rough calculation indicates that the extra slip amounts to only 5 pct of the total.

It may be noted that the use of small strain equations [35] would have led to a value of $\tan \theta_{32}$ $= [(h_1/h_0) - 1]/\sqrt{2}$. As shown in Fig. 6, this value errs by a factor of about two after 50 pct thickness reduction.

DOUBLE GLIDE IN TENSION—EQUAL PRIMARY AND CONJUGATE SLIP

The tensile axis of a single crystal which initially deforms by single slip generally rotates toward the slip direction until the [001]-[$\bar{1}11$] symmetry line is reached; see Fig. 1. Equal slip on both primary, (111)[$\bar{1}01$], and conjugate, ($\bar{1}\bar{1}1$)[011], systems will then rotate the tensile axis along the symmetry line toward the [$\bar{1}12$] final position. Since these slip systems are the same as those operated in the previous (110)[$\bar{1}12$] compression case, the same deformation gradient matrix [33] may be used. In the present case, however, the initial elongation direction is not at the [$\bar{1}12$] position, but instead at ϵ_0 from it, say. We are interested in the relationship between tensile elongation, amount of glide, and lattice rotation as deformation proceeds by double glide.

Letting [110], [$\bar{1}1\bar{1}$], [$\bar{1}12$] be coordinate axes as before, the deformation gradient matrix from [33] is

$$F = \begin{bmatrix} e^{-\varphi} & 0 & 0 \\ 0 & 1 & 0 \\ 0 & \frac{1}{\sqrt{2}}(1 - e^{\varphi}) & e^{\varphi} \end{bmatrix} \qquad [37]$$
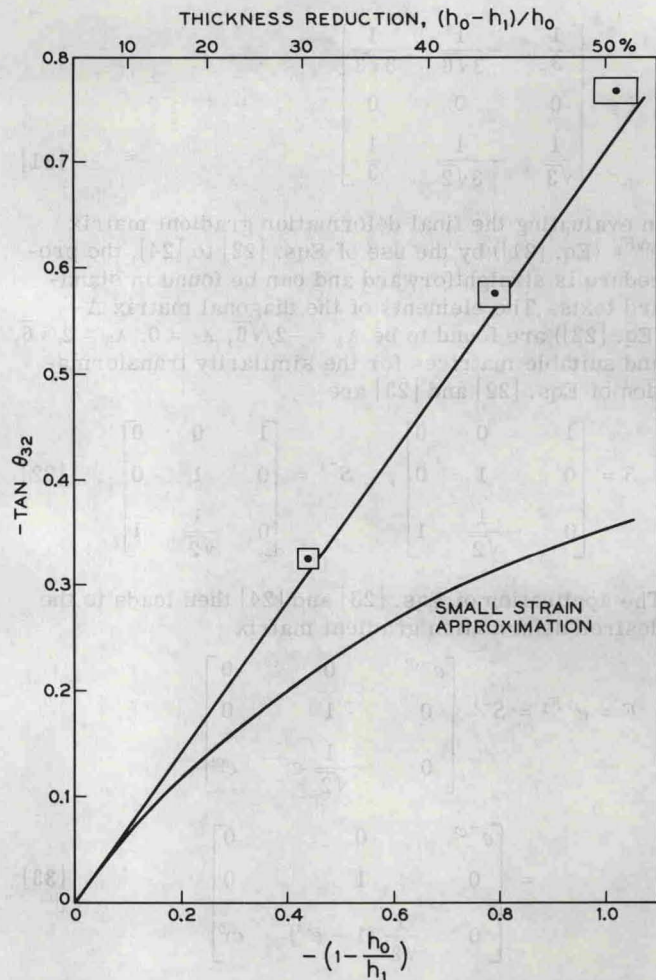
Fig. 6—Plot of $\tan \theta_{32}$ vs $(1 - h_1/h_0)$ for (110)[$\bar{1}12$] compression. Straight line is according to theory, assuming only (11$\bar{1}$)[011] and (111)[$10\bar{1}$] slip. Measured points from experiment on Permalloy single crystal. Size of square containing measured point indicates range of errors in measurement.

For a tensile axis initially at ϵ_0 degrees from [$\bar{1}12$] and toward [001], the unit vector **P** along this axis is

$$\mathbf{P} = -\sin \epsilon_0 \mathbf{i}_2 + \cos \epsilon_0 \mathbf{i}_3 \qquad [38]$$

or

$$P_1 = 0, \quad P_2 = -\sin \epsilon_0, \quad P_3 = \cos \epsilon_0$$

Let the tensile axis move to a position ϵ_1 deg from [$\bar{1}12$] after the deformation with the line **p** along this axis being

$$\mathbf{p} = -\sin \epsilon_1 \mathbf{i}_2 + \cos \epsilon_1 \mathbf{i}_3 \qquad [39]$$

or

$$p_1 = 0, \quad p_2 = -\sin \epsilon_1, \quad p_3 = \cos \epsilon_1$$

From Eq. [6], which relates the direction cosines of the two lines, we have

$$\lambda_\mathbf{p} p_2 = \frac{\partial x_2}{\partial X_1} P_1 + \frac{\partial x_2}{\partial X_2} P_2 + \frac{\partial x_2}{\partial X_3} P_3$$

or

$$-\lambda_\mathbf{p} \sin \epsilon_1 = -\sin \epsilon_0$$

or